JPn

Neuroscience

The Journal of Physiology

Generation of striatal projection neurons extends into the neonatal period in the rat brain

Jordan Wright[1,2], Davor Stanic[1,2] and Lachlan H. Thompson[1,2]

[1] *Centre for Neuroscience, University of Melbourne, Parkville, Australia*
[2] *Florey Neuroscience Institute, University of Melbourne, Parkville, Australia*

Key points

- Studies on postnatal neurogenesis as a constitutive physiological process have largely focused on the adult brain.
- This study identifies and characterises a continued period of striatal neurogenesis under normal physiological conditions in the neonatal brain.
- Birth-dating studies show a peak production of striatal projection neuron generation at post-natal day 0 that declines sharply within the first postnatal week.
- New striatal projection neurons integrate appropriately into existing circuitry through target-directed innervation of appropriate sub-striatal structures.
- The results are highly relevant for the development of regenerative strategies for neonatal brain repair.

Abstract Substantial advances have been made in the last decade on our understanding of the basic physiology underlying neurogenesis in the postnatal mammalian brain. The bulk of the work in this area has been based on analysis of the adult brain. Relatively less is known about the capacity for neurogenesis in specific structures within the neonatal brain. Here we report that the production of medium spiny striatal projection neurons extends into the early neonatal period under normal physiological conditions in the rat brain. Birth-dating of newborn cells with bromodeoxyuridine at postnatal days 0, 2 and 5 showed a peak production close to birth, which sharply declined at the later time-points. Additionally, there was a low-level but stable contribution of neurons with interneuron identity over the same time-period. Importantly, retroviral labelling of new striatal projection neurons with green fluorescent protein showed long-term survival and terminal differentiation with characteristic morphology, including highly elaborated spiny dendrites, and appropriate axonal targeting of the globus pallidus and midbrain. This latent period of striatal neurogenesis in the early neonatal brain represents an interesting target for regenerative approaches aimed at restoring striatal circuitry in perinatal pathologies, such as hypoxic and ischaemic damage associated with cerebral palsy.

Introduction

Striatal projection neurons form an important part of basal ganglia circuitry in the form of inhibitory pathways that innervate sub-striatal targets, including the globus pallidus and the substantia nigra (Gerfen & Wilson, 1996). Disruption of these signalling pathways is common to a number of neurological conditions, including Huntington's disease (Lange *et al.* 1976; Reiner

et al. 1988), stroke (Arvidsson *et al.* 2002) and hypoxic damage linked to cerebral palsy (Mallard *et al.* 1995). The limited ability of the postnatal brain to replace projection neurons means that the loss of striatal circuitry has permanent functional consequences, commonly incorporating movement disorders (Janavs & Aminoff, 1998). Substantial advances in our understanding of the physiology underlying neurogenesis in the postnatal brain have fuelled interest into strategies for encouraging replacement of neurons after injury. Fundamental to the successful development of such approaches is a basic understanding of the intrinsic capacity of the brain to generate specific neuronal subtypes of interest under both normal physiological as well as pathological conditions.

Transplantation and birth-dating experiments have shown that striatal projection neurons are generated from ventricular zone progenitors in the lateral ganglionic eminence (LGE) during embryogenesis, with a peak phase of production between embryonic days 12–17 (E12–17) in the rodent brain (van der Kooy & Fishell, 1987; Deacon *et al.* 1994; Olsson *et al.* 1995, 1998). As development proceeds, these progenitors cease to produce striatal projection neurons and instead contribute interneuron subtypes destined for the olfactory bulb during later stages of embryogenesis and persisting throughout adulthood (Luskin, 1993; Alvarez-Buylla & Garcia-Verdugo, 2002; Sui *et al.* 2012). Although recent studies have shown that new neurons can in fact appear in the intact adult striatum of various species, including rats (Dayer *et al.* 2005), rabbits (Luzzati *et al.* 2006) and primates (Bedard *et al.* 2002), only interneuron subtypes have been described (for review, see Bonfanti & Peretto, 2011). Under normal physiological conditions, the adult brain does not appear to retain the ability to generate striatal projection neurons.

Thus, while the spectrum of neurogenesis for striatal projection neurons spans peak production embryonically to cessation in the adult brain, relatively less is known about the capacity for dividing cells in the early postnatal brain to generate striatal neurons. There are topographically organised patterns of cell division in the neonatal striatum (Stopczynski *et al.* 2008), and birth-dating studies have shown that new striatal projection neurons are generated up until close to birth (E20) in the rat brain (van der Kooy & Fishell, 1987). Here we sought to identify the incidence and pattern of striatal neurogenesis in the neonatal rat brain through birth-dating with the thymidine analogue bromo-deoxyuridine (BrdU) and retroviral delivery of green fluorescent protein (GFP). Detection of BrdU, combined with phenotypic markers of cellular identity, allowed us to map the general pattern of cell division across the striatum at different neonatal time-points and to assess the proportion of neuronal differentiation. Importantly, the cytoplasmic distribution of GFP allowed us to characterise new-born cells in the neonatal brain with fine morphological detail.

Together with the BrdU data, the results show that the production of medium spiny striatal neurons persists in the early neonatal period. Conceptually, this may have important implications for the design of regenerative approaches for pathological conditions affecting the striatum during this period, such as neonatal hypoxia and/or ischaemia. It suggests that therapeutic interventions may focus on augmenting a phenomenon that occurs under normal physiological conditions, rather than seeking to re-establish production of striatal projection neurons during the post-neurogenic period.

Methods

Ethical approval

The use of animals in this study conformed to the Australian National Health and Medical Research Council's published Code of Practice for the Use of Animals in Research, and experiments were approved by the Florey Neuroscience Institutes animal ethics committee (no. 09-105).

Animals and *in vivo* procedures

Time-mated, pregnant Sprague–Dawley rats were housed under a 12 h light/dark cycle with *ad libitum* access to food and water. A total of 20 newborn rats (corresponding to three litters) were taken for surgical procedures at postnatal day 0 (P0), 2 or 5. All surgical procedures were performed using a cooled, Cunningham adapter (Stoelting, Germany) fitted to a stereotaxic frame (Kopf, Germany). Hypothermic anaesthesia was induced by placing each neonate in ice for 5 min and maintained by adding dry ice to absolute ethanol in a reservoir built into the Cunningham adaptor stage. Under deep anaesthesia, five animals from each postnatal time-point received 4 μl BrdU (Sigma) solution (20 mg ml^{-1} in 0.9% sterile saline) over 2 min into the right lateral ventricle (0.5 mm anterior and 1.1 mm lateral to bregma and 2.5 mm below the dural surface). At the P0 time-point, an additional five rats received 1 μl of moloney murine retrovirus encoding GFP constitutively under the CAG promoter (1 × 10^8 transducing units ml^{-1}; kind gift from Professor Deniz Kirik, Lund University). The injections were performed using a fine glass capillary fitted to a 5 μl microsyringe (SGE Analytical Sciences, Australia), and the cannula was left in place for 2 min before withdrawal to prevent backflow of the injected material. To ensure robust BrdU-labelling of dividing cells, the animals also received a single 50 μl I.P. injection of the same BrdU solution (approximately 150 mg kg^{-1}) at the time of surgery. The

neonates revived spontaneously with recovery of physiological body temperature through handling and the use of a heat-lamp, and were returned to their mothers. We also treated adult (250 g) female Sprague–Dawley rats with I.P. injections of BrdU. Initial experiments where animals received a single injection at 150 mg kg^{-1} showed very low numbers of labelled cells (not shown). We therefore treated adult animals ($n = 5$) with a course of 50 mg kg^{-1} I.P. injections every 12 h as previously described (Arvidsson *et al.* 2002).

Tissue preparation

At 4 weeks (BrdU groups) or 12 weeks (retroviral GFP groups) after surgery, the animals received a lethal dose of pentobarbitone and were transcardially perfused with 50 ml saline (0.9% w/v) followed by 200–250 ml paraformaldehyde (PFA; 4% w/v in 0.1 M PBS). The brains were removed, post-fixed a further 2 h in PFA and cryoprotected in sucrose (25% w/v in 0.1 M PBS). Brains were sectioned in the coronal plane in a 1:12 series at a thickness of 30 μm on a freezing microtome (Leica, Germany).

Immunohistochemistry

Immunohistochemical procedures were performed as previously described (Thompson *et al.* 2005). For BrdU-labelling, the free-floating tissue sections were incubated in 50% de-ionised formamide (in 0.1 M PBS) for 2 h at 65°C, washed for 15 min three times in PBS, incubated in 2 M HCl for 30 min at 37°C, washed for 15 min in sodium borate buffer (pH 8.0) before a final 3 × 15 min washes in PBS.

The free-floating sections were incubated overnight at room temperature with primary antibodies diluted in 0.1 M PBS containing 5% normal serum and 0.25% Triton X-100 (Amereso, USA). Secondary antibodies diluted in PBS with Triton X-100 and 2% normal serum were applied for 2 h at room temperature. The primary-secondary antibody complex was visualised by peroxidase-driven precipitation of diaminobenzidine (DAB) or conjugation of a fluorophore. Fluorescent slide-mounted sections were cover-slipped with fluorescent mounting medium (DAKO, USA). DAB-labelled sections were dehydrated in alcohol and xylene, and cover-slipped with DePex mounting medium (BDH Chemicals, UK).

Primary antibodies and dilution factors were as follows: rat anti-BrdU (1:300; Axyll Laboratories, Westbury, USA), mouse anti-calretinin (1:1000; Swant, Switzerland), rabbit anti-Darpp32 (1:500; Santa Cruz Biotechnology, Santa Cruz, USA), chicken anti-GFP (1:1000; AbCam, Cambridge, USA), rabbit anti-GFP (1:20,000; AbCam) and mouse anti-NeuN (1:200; Millipore Billerica, USA). For DAB-based detection of GFP, a biotinylated goat anti-rabbit secondary antibody (Vector Laboratories, USA) was subsequently conjugated with streptavidin-HRP using the Vectastain ABC Elite kit (Vector Laboratories). For immunofluorescence, species-specific secondary antibodies generated in donkey and conjugated with the Dylight range of fluorophores with various peak emission wavelengths including 488 nm, 549 nm and 633 nm were used at a dilution of 1:500 (Jackson Immunoresearch, USA).

Imaging

Fluorescent images were captured using a Zeiss Meta laser-scanning confocal upright microscope. The intensity and contrast of each image was enhanced through adjustment of the levels in individual colour channels using Photoshop (Adobe) to optimally represent the immunohistochemistry observed through the microscope. Brightfield images of DAB-labelled GFP staining were captured using a Leica DM6000 B upright light microscope equipped with a motorised stage and de-convolution software.

Quantification and statistics

Immunohistochemistry (for either BrdU/NeuN/Darpp32 or BrdU/NeuN/calretinin was analysed in three(sections spanning the bulk of the anterior head of the striatum (bregma +1.7 mm, +0.7 mm, −0.3 mm), but not including the caudal tail (see Fig 3). Each BrdU$^+$ cell in the striatum was counted and individually inspected for co-labelling for NeuN, Darpp32 or calretinin. Cells assessed as co-labelled were further analysed on the z-axis for confirmation. The average number of BrdU$^+$ cells or cells co-labelled with phenotypic markers was compared between experimental groups (P0, $n = 4$; P2, $n = 5$; P5, $n = 4$) using one-way ANOVA with *post hoc* correction (Bonferonni) for multiple comparisons. The total number of cells in the head of the striatum (between +1.7 mm and −0.3 mm relative to bregma) was estimated by extrapolation according to the series interval (12) and the number of sections quantified in each series (3/5). Cell numbers for the different experimental groups are reported as the mean ± SD.

Results

Acute BrdU treatment labelled dividing cells throughout both hemispheres, at all of the neonatal time-points, and these cells could be detected 4 weeks later through immunohistochemistry (Fig. 1). Quantification of BrdU$^+$ cells across three sections spanning the striatum (bregma +1.7 mm, +0.7 mm, −0.3 mm) in each brain revealed a similar number of cells in the P0 ($12.59 \pm 0.3 \times 10^3$)

and P2 ($12.17 \pm 0.18 \times 10^3$) groups, but a significantly greater number in the P5 ($21.44 \pm 0.55 \times 10^3$) group ($P < 0.01$; Fig. 1*D*). The pattern of BrdU$^+$ cells showed intense labelling within the subventricular zone (SVZ) and more diffuse labelling throughout the striatal parenchyma, which appeared most prominent in the ventral striatum (Fig. 1*B* and *C*). Adult animals that received 2 weeks of BrdU treatment had an average of $4.1 \pm 0.17 \times 10^4$ BrdU-labelled cells in the striatum. The highest density of BrdU labelling was again in the SVZ and the adjacent rostral migratory stream (RMS; not shown).

Double-labelling with NeuN showed that many of the dividing cells at P0 became neurons ($1.66 \pm 0.51 \times 10^3$; Fig. 2). This number declined significantly ($P < 0.005$) for dividing cells labelled at the later, P2 ($0.38 \pm 0.14 \times 10^3$)

and P5 ($0.28 \pm 0.11 \times 10^3$) time-points. The rate of striatal neurogenesis, determined as the fraction of BrdU$^+$ cells co-labelled with NeuN, also declined from $12 \pm 1.78\%$ at P0 to $3.16 \pm 1.1\%$ at P2 and $1.57 \pm 0.82\%$ at P5. We did not detect a single NeuN$^+$ cell from $>10^4$ BrdU cells examined in the striatal parenchyma across five adult animals treated with BrdU. We did observe the presence of BrdU$^+$/calretinin$^+$/NeuN$^-$ cells, and these were located primarily in close proximity to the SVZ and RMS (not shown).

Immunohistochemistry for the dopamine- and cyclic AMP-regulated phosphoprotein of 32 kDa (Darpp32) revealed $51.18 \pm 15.49\%$ of the new neurons had acquired phenotypic features consistent with a striatal projection neuron identity at P0. This figure declined for dividing
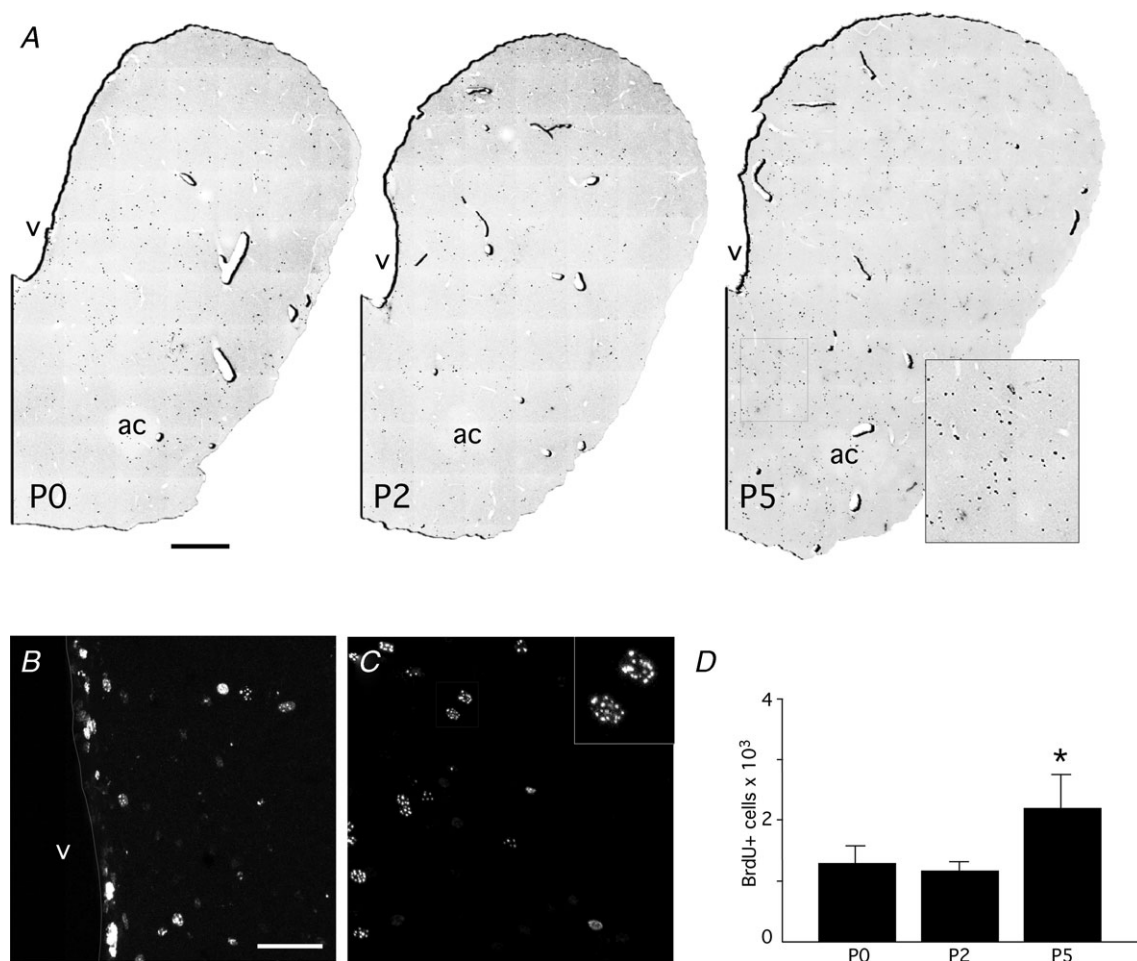
Figure 1. Birth-dating with bromodeoxyuridine (BrdU) in the neonatal brain identifies newborn cells in the striatum
Representative sections showing immunohistochemistry for BrdU 4 weeks after administration at P0, P2 or P5 reveal extensive labelling in the striatum (*A*; boxed area in P5 section expanded for detail). The SVZ contained the highest density of BrdU$^+$ cells (*B*), which were more diffusely distributed throughout the striatal parenchyma, often with a punctate appearance (*C*; boxed area enlarged for detail). One-way ANOVA showed that the striatum of animals injected at P5 ($n = 4$) contained significantly more BrdU$^+$ cells then the P0 ($n = 4$) and P2 ($n = 4$) groups (*D*; $P < 0.01$). Abbreviations: ac, anterior commissure; P0/2/5, postnatal day 0/2/5; v, lateral ventricle. Scale bar: 1 mm (*A*); 50 μm (*B* and *C*).

cells labelled at the later time-points, with $38.36 \pm 15.65\%$ and $36.11 \pm 18.43\%$ of BrdU$^+$/NeuN$^+$ cells identified as Darpp32$^+$ in the P2 and P5 groups, respectively. While this difference was not in itself statistically significant, it translated to a significant ($P < 0.01$) reduction in the *absolute* number of Darpp32-labelled neurons at the later time-points (148 ± 98 at P2 and 105 ± 62 at P5), compared with 890 ± 421 at P0 (Fig. 2). Figure 3 shows the distribution of BrdU-labelled NeuN$^+$ and NeuN$^+$/Darpp32$^+$ neurons within the striatum of representative sections from all time-points. While there was no specific anatomical pattern to the Darpp32$^+$ fraction, the overall pattern of neurogenesis showed a preferential distribution in the anterior and ventro-medial aspects of the striatum (not shown). None of the cells labelled with BrdU in the adult brain was found to co-express Darpp32.

We also looked at the incidence of differentiation into calretinin$^+$ interneurons within the striatal parenchyma. Similarly, there was no specific anatomical pattern of calretinin$^+$ distribution within the

BrdU$^+$/NeuN$^+$ population (not shown). Compared with differentiation into Darpp32$^+$ phenotypes, the numbers of BrdU$^+$/NeuN$^+$/calretinin$^+$ cells were overall lower and more variable between animals, but more closely matched across the different postnatal time-points examined: 30 ± 47.6 at P0; 35 ± 41.23 at P2; and 40 ± 48.99 at P5 (Fig. 2). The relatively stable numbers across each time-point probably reflect that while the overall incidence of neurogenesis declined, there was an increase (n.s.) in the fraction of neurons that acquired a calretinin$^+$ identity: $1.48 \pm 2.36\%$ from the P0 group; $8.35 \pm 10.23\%$ from P2; and $20.83 \pm 20\%$ from the P5 group. The generation of new calretinin$^+$ neurons persisted into adulthood with an average of 140 ± 37.41 calretinin$^+$/BrdU$^+$ cells per striatum. Almost all of these cells were found in close proximity to the SVZ or RMS, and did not co-express NeuN, suggesting an early neuroblast identity.

To further characterise newly generated neurons in the neonatal striatum, particularly the potential for generation of striatal projection neurons, an additional group of
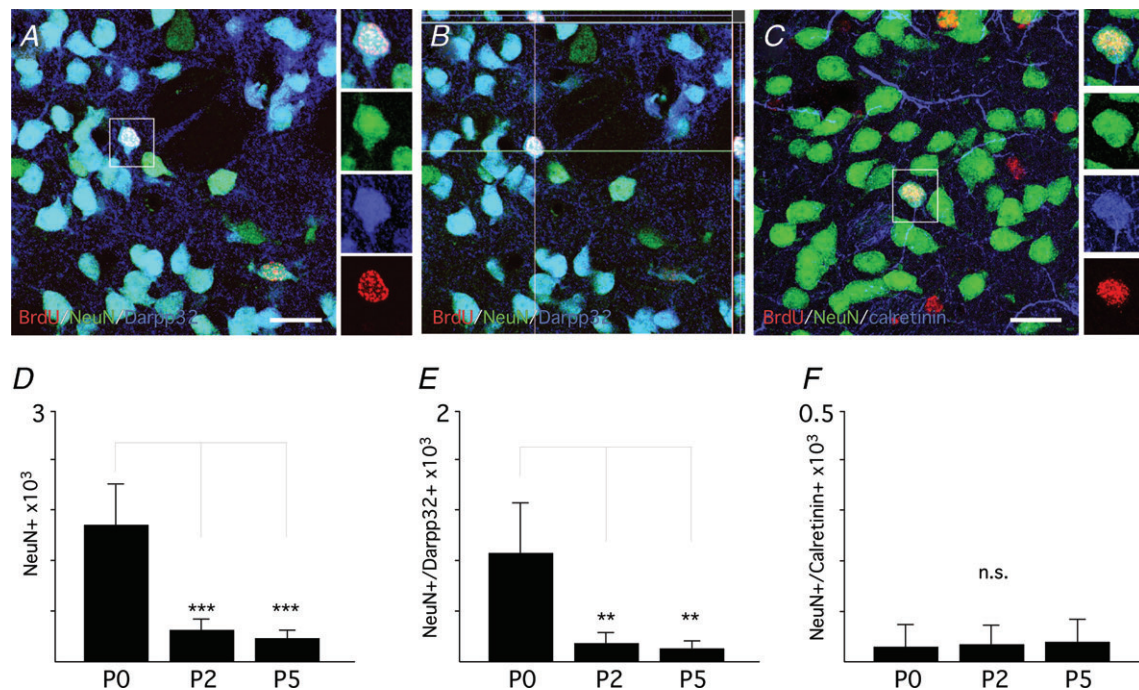
Figure 2. Newborn cells in the postnatal brain differentiate into striatal neurons
A, immunohistochemistry for bromodeoxyuridine (BrdU), NeuN and Darpp32 illustrates the generation of new neurons with striatal projection phenotype in the neonatal brain (boxed area shown as individual colour channels). *B*, confirmation of co-registration of immunolabelled proteins in the same cell was achieved by orthogonal re-construction on the *z*-axis. *C*, new BrdU$^+$/NeuN$^+$ with interneuron identity were observed based on co-labelling with calretinin (boxed area shown as individual colour channels). *D*, significantly more BrdU$^+$/NeuN$^+$ cells were observed at the P0 ($n = 4$) time-point compared with the later P2 ($n = 5$) and P5 ($n = 4$) time-points (one-way ANOVA; $P < 0.005$). *E*, significantly more BrdU$^+$/NeuN$^+$/Darpp32$^+$ cells were observed at the P0 ($n = 4$) time-point compared with the later P2 ($n = 5$) and P5 ($n = 4$) time-points (one-way ANOVA; $P < 0.01$). *F*, the number of BrdU$^+$/NeuN$^+$/calretinin$^+$ cells was not significantly different between the P0 ($n = 4$), P2 ($n = 5$) and P5 ($n = 4$) groups based on one-way ANOVA. Abbreviation: P0/2/5, postnatal day 0/2/5. Scale bar: 20 μm (*A* and *B*); 20 μm (*C*).

animals ($n = 5$) received a unilateral, intraventricular injection of a replication deficient moloney murine leukaemia virus encoding GFP constitutively under the CAG promoter at P0. A survival period of 12 weeks was chosen to allow sufficient time for differentiation and acquisition of mature morphological features, including axonal growth. Immunohistochemistry for GFP showed extensive labelling of cells throughout the cortex (not shown) and striatum (Fig. 4A) of the injected hemisphere, as well as GFP+ cells more sparsely distributed in the contralateral hemisphere (not shown). Numerous GFP+ cells with a simple, rounded morphology could consistently be found in the SVZ on the lateral side of the injected ventricle (Fig. 4B). The vast majority of GFP+ cells, however, were found in the striatal parenchyma with morphological characteristics of mature astrocytes, including both protoplasmic and fibrous astrocytic morphologies (Fig. 4C). Interestingly, we also found numerous GFP+ cells with striatal projection neuron morphology (Fig. 4D), including characteristically spiny dendrites (Fig. 4E). The majority of these cells were found in ventral parts of the striatum, particularly in

and around the core and shell of the nucleus accumbens surrounding the anterior commissure. Darkfield imaging showed the presence of GFP+ fibres in appropriate target areas for striatal projection neurons, including the globus pallidus and, to a lesser degree, the substantia nigra (Fig. 4F and G). Double-labelling showed that GFP+ cells with striatal projection neuron morphology co-expressed Darpp32 (Fig. 5A). Other GFP+ neurons without medium spiny neuron morphology could also be observed and at least some of these cells co-expressed the interneuron marker calretinin (Fig. 5B), particularly the smaller sized neurons.

Discussion

At all neonatal time-points investigated, as well as in adult animals, administration of BrdU resulted in robust labelling of cells that could be visualised by immunohistochemistry 4 weeks later. In the neonatal animals the average number of BrdU+ cells in the striatum was greatest in animals injected at the latest (P5) time-point. This may
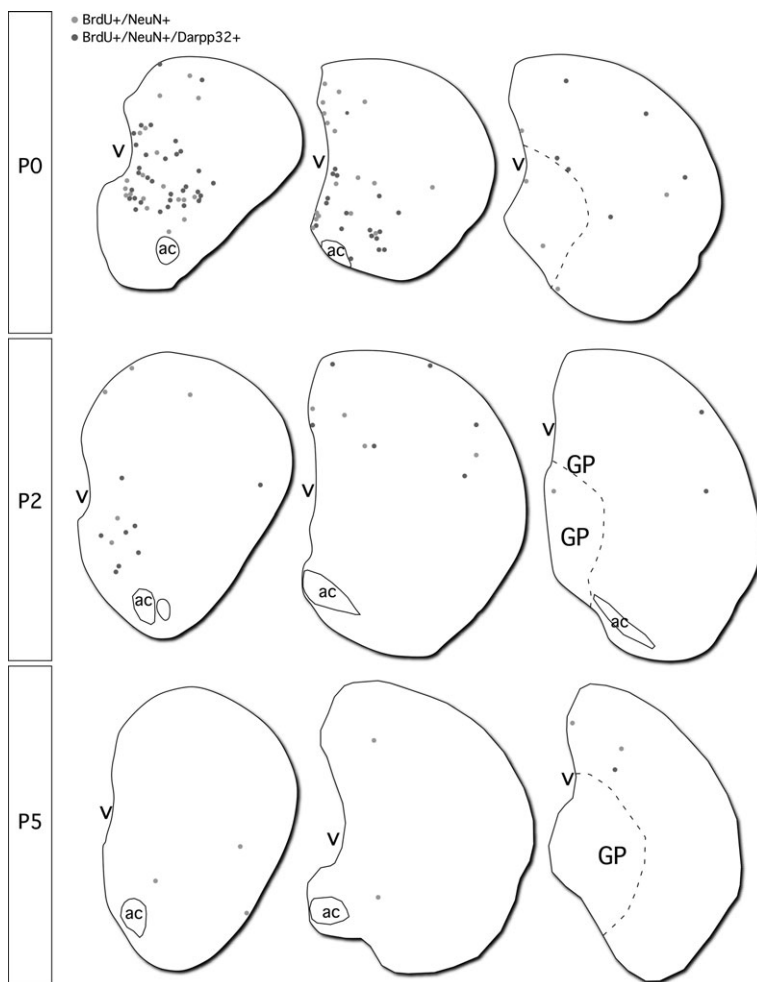
Figure 3. Striatal distribution of neurons generated in the neonatal brain 4 weeks after birth-dating
The locations of BrdU+/NeuN+ (grey) and BrdU+/NeuN+/Darpp32+ (black) cells within representative striatal sections from each birth-dating time-point were mapped by annotating automated photo-montages captured by confocal microscopy. Each BrdU+ striatal cell was inspected for co-labelling for NeuN and Darpp32. Abbreviations: ac, anterior commissure; GP, globus pallidus; P0/2/5, postnatal day 0/2/5; v, lateral ventricle.

result from a number of variables including heterogenous, and not necessarily linear, growth dynamics of specific brain structures during the neonatal period. For example, the rate of gliogenesis is known to increase significantly between the first and second week of life in the neonatal rat brain (Bandeira *et al.* 2009). Furthermore, although the rate of cell proliferation may be similar across the neonatal ages examined, there may be differences in the fraction of labelled cells that survive. It has been well-established that there is significant apoptotic cell loss throughout the brain, including the striatum (Fishell & van der Kooy, 1991; Maciejewska *et al.* 1998), during the early neonatal period.

Our objective in this study was to assess the capacity of the early postnatal brain to generate striatal projection neurons. Recent reports have provided convincing evidence that postnatal forebrain neurogenesis extends beyond the well-characterised generation of neuroblasts in the SVZ that populate the olfactory bulb via the RMS (De Marchis *et al.* 2004; Inta *et al.* 2008; Sanai *et al.* 2011; for review, see Bonfanti & Peretto, 2011). In neonatal mice, experiments using fluorescent dyes (De

Marchis *et al.* 2004) as well as transgenic and retroviral lineage tracing (Inta *et al.* 2008) show additional migratory pathways for SVZ neuroblasts resulting in GABAergic interneurons in various forebrain structures, including the cortex, striatum, olfactory tubercle and Islands of Calleja. Similarly in the early postnatal human brain, a recent study has described the transient existence of a medial migratory stream of neuroblasts that diverges from the RMS, possibly contributing new interneurons to the ventro-medial pre-frontal cortex (Sanai *et al.* 2011). All of these studies have focussed on the addition of interneuron subtypes to the postnatal forebrain. Here we report that forebrain neurogenesis in neonatal rats includes the addition of new striatal projection neurons.

Double-labelling of newborn, BrdU$^+$ cells with the pan-neuronal marker, NeuN, revealed ongoing striatal neurogenesis that tapers off significantly within the first 5 postnatal days. A substantial proportion ($51 \pm 15\%$) of the new neurons (NeuN$^+$) born at P0 appeared to have adopted a striatal projection neuron phenotype by 4 weeks, based on co-expression of Darpp32. By 5 days postnatal, however, very few newborn cells gave rise to
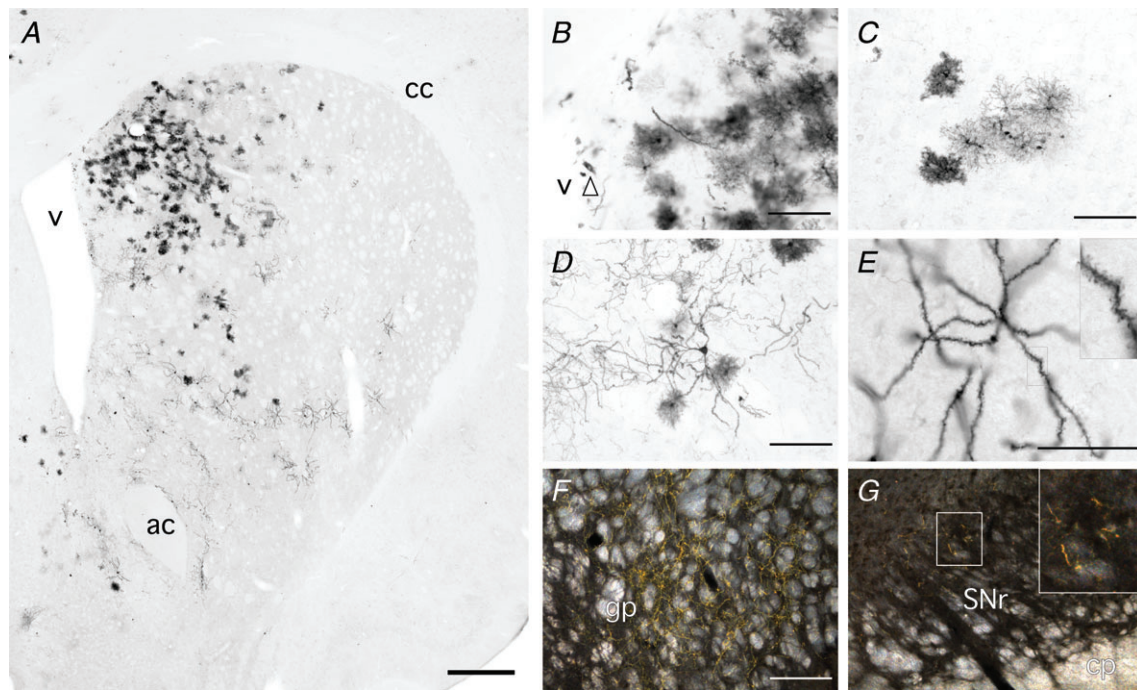
Figure 4. Retroviral delivery of GFP identifies newborn cells in the neonatal brain with morphological detail
A, immunohistochemistry for GFP 12 weeks after retroviral delivery at P0 revealed extensive labelling throughout the striatum. *B*, many GFP$^+$ cells with unelaborated morphology were consistently seen in the SVZ (arrowhead). *C*, the dominant morphological phenotype was astrocytic, including both protoplasmic (left of panel, darker cells) and fibrous profiles. *D*, cells with neuronal morphology were clearly identified and were often found in ventral areas of the striatum. *E*, the most common neuronal morphology was of medium spiny neurons with highly elaborated spiny dendrites (boxed area enlarged as inset). Darkfield imaging showed GFP$^+$ fibres (yellow) in the globus pallidus (*F*) and midbrain (*G*) of some animals (boxed area in *G* enlarged as inset). Abbreviations: ac, anterior commissure; cc, corpus callosum; cp, cerebral peduncle; gp, globus pallidus; SNr, substantia nigra; v, lateral ventricle. Scale bars: 1 mm (*A*); 100 μm (*B–D*); 50 μm (*E*); 200 μm (*F* and *G*).

Darpp32^{+} neurons. This was a reflection of both the lower overall rate of striatal neurogenesis and also a lower proportion of new neurons co-labelling with Darpp32 at the later time-point. Importantly, retroviral labelling of newborn cells with GFP allowed us to characterise the phenotype of striatal neurons generated at P0 with fine morphological detail. Many of the GFP neurons displayed the characteristic profile of striatal projection neurons, including dendritic trees heavily adorned with spiny processes. Furthermore, the cytoplasmic GFP label throughout the axonal process showed that the new neurons were capable of appropriate structural integration, including long-distance innervation of the globus pallidus and midbrain.

These results suggest that the period of normal development of the striatal neuron projection system, known to occur up until close to birth (van der Kooy & Fishell, 1987), persists, at least for a short time, in the early postnatal brain. Although the present results do not allow us to conclude the origin of the newborn striatal neurons, we speculate that they are derived from the SVZ as a continuum of the embryonic developmental process whereby striatal projection neurons are generated from SVZ progenitors in the LGE (Deacon *et al.* 1994; Olsson *et al.* 1998; Wichterle *et al.* 2001; Stenman *et al.* 2003). It is worth noting, however, studies in rabbits have demonstrated the local production of new neurons (albeit calretinin[+] interneurons) in the striatal parenchyma of the postnatal brain (Luzzati *et al.* 2006). In the interest of developing therapeutic approaches that exploit neonatal striatal neurogenesis, it will be important to more precisely identify the origins of the new striatal projection neurons identified in the present study.

Only a minor proportion of all BrdU^{+} cells were found to be neurons by co-labelling with NeuN. A significant proportion of the NeuN-negative population likely represents cells that become astrocytes or remain in an immature progenitor state. We have previously reported that many of the proliferating cells in the postnatal striatum are local progenitors that give rise to mature glial cell types or remain unidentified (Irvin *et al.* 2008). In support of this, the major morphological phenotype of GFP^{+} cells following retroviral-GFP injection at P0 was astrocytic. Many of the BrdU[+]/NeuN[+] did not co-express Darpp32 and, while this may reflect lack of maturity in some cells at the 4 week time-point, it also suggests that not all of the newborn striatal neurons adopt a projection neuron identity. Co-labelling with calretinin showed that at least some become interneurons. Interestingly, unlike the generation of new Darpp32^{+} neurons, which declined significantly across the P0, P2 and P5 neonatal time-points, the overall percentage of NeuN^{+} cells expressing calretinin was comparatively smaller at each time-point and *increased* over time. This is consistent with the idea that, while production of striatal projection neurons ceases during the early postnatal period, the generation of certain classes of striatal interneurons can persist into adulthood, as recently reported (Dayer *et al.* 2005).

The transient persistence of striatal projection neurogenesis in the postnatal brain provides an interesting target for regenerative therapies for neonatal brain damage. Perinatal ischaemia, hypoxia and intraventricular haemorrhage are leading causes of cerebral palsy (for review, see Titomanlio *et al.* 2011; Bennet *et al.* 2012), and can involve damage to the striatum (Mallard *et al.* 1995) as a likely cause of deficits in motor function. In the adult brain, conclusions on the ability of newborn neurons to acquire a medium spiny projection identity following damage have been mixed. Initial work in this area reported that a small fraction of the surviving neurons express markers consistent with medium spiny projection identity, including Darpp32 (Arvidsson *et al.* 2002; Parent *et al.* 2002), while a subsequent study has reported that new neurons diverted from the SVZ to the damaged striatum maintain their normal differentiation potential as olfactory bulb interneurons (Liu *et al.* 2009).

A maintained intrinsic ability for differentiation into medium spiny projection neurons in the neonatal brain may represent a more promising target for striatal repair. A number of studies have reported that ischaemic-hypoxic damage to the neonatal striatum results in the recruitment of new striatal neurons (Plane *et al.* 2004; Iwai *et al.* 2007; Yang *et al.* 2008; Im *et al.* 2010). The work of Yang *et al.* (2008) looked specifically at the resulting neuronal phenotypes and found no differentiation into Darpp32^{+} neurons, but rather that the majority of new cells acquired a calretinin[+] interneuron identity. In agreement with the conclusions of Liu *et al.* (2009), the authors suggest that neurons reaching the damaged striatum are pre-committed to a calretinin[+] interneuron fate. In light of the present results under normal physiological
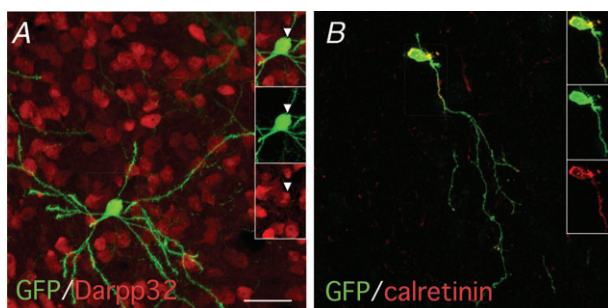
Figure 5. Morphological and molecular features of striatal neurons 12 weeks after injection of retroviral green fluorescent protein (GFP) into the lateral ventricle of neonatal rats

A, neurons with medium spinal projection morphology also co-labelled with Darpp32. *B*, smaller neurons, lacking spiny dendrite morphology, often co-labelled with calretinin. Scale bar: 20 μm.

conditions, this may be due to a selective vulnerability of newborn striatal projection neurons in a pathological environment in the neonatal striatum. Alternatively, the results of Yang *et al.* (2004) may reflect that the birth-dating at P9 was done after the latest (P5) time-point investigated in the present study, and therefore after the final stages of the neurogenic period for striatal projection neurons. Additional studies of neonatal striatal injury with birth-dating performed at earlier time-points are required to investigate this possibility.

In summary, we report here that medium striatal projection neurons are generated in the neonatal rat brain under normal physiological conditions. These neurons survived up until 12 weeks, a time when the rodent brain is fully developed, and had molecular and morphological features appropriate for terminally differentiated medium spiny projection neurons, including long-distance terminal innervation of appropriate targets in the globus pallidus and midbrain. This has not previously been demonstrated in the adult brain, and thus the early neonatal period may provide a unique window for therapeutic intervention aimed at repairing the damaged striatum. Previous studies have shown that growth factors administered at P9 or 6 weeks after neonatal ischaemia can stimulate neurogenesis of non-Darpp32$^+$ neurons (Iwai *et al.* 2007; Im *et al.* 2010). Applying this strategy at earlier time-points, during an active phase of neurogenesis for striatal projection neurons may be an effective approach for replacing damaged striatal projection circuitry and restoring associated functional deficits in neonatal brain damage, such as occurs in cerebral palsy.

References

Alvarez-Buylla A & Garcia-Verdugo JM (2002). Neurogenesis in adult subventricular zone. *J Neurosci* **22**, 629–634.

Arvidsson A, Collin T, Kirik D, Kokaia Z & Lindvall O (2002). Neuronal replacement from endogenous precursors in the adult brain after stroke. *Nat Med* **8**, 963–970.

Bandeira F, Lent R & Herculano-Houzel S (2009). Changing numbers of neuronal and non-neuronal cells underlie postnatal brain growth in the rat. *Proc Natl Acad Sci U S A* **106**, 14108–14113.

Bedard A, Cossette M, Levesque M & Parent A (2002). Proliferating cells can differentiate into neurons in the striatum of normal adult monkey. *Neurosci Lett* **328**, 213–216.

Bennet L, Tan S, Van den Heuij L, Derrick M, Groenendaal F, van Bel F, Juul S, Back SA, Northington F, Robertson NJ, Mallard C & Gunn AJ (2012). Cell therapy for neonatal hypoxia-ischemia and cerebral palsy. *Ann Neurol* **71**, 589–600.

Bonfanti L & Peretto P (2011). Adult neurogenesis in mammals–a theme with many variations. *Eur J Neurosci* **34**, 930–950.

Dayer AG, Cleaver KM, Abouantoun T & Cameron HA (2005). New GABAergic interneurons in the adult neocortex and striatum are generated from different precursors. *J Cell Biol* **168**, 415–427.

De Marchis S, Fasolo A & Puche AC (2004). Subventricular zone-derived neuronal progenitors migrate into the subcortical forebrain of postnatal mice. *J Comp Neurol* **476**, 290–300.

Deacon TW, Pakzaban P & Isacson O (1994). The lateral ganglionic eminence is the origin of cells committed to striatal phenotypes: neural transplantation and developmental evidence. *Brain Res* **668**, 211–219.

Fishell G & van der Kooy D (1991). Pattern formation in the striatum: neurons with early projections to the substantia nigra survive the cell death period. *J Comp Neurol* **312**, 33–42.

Gerfen CR. & Wilson CJ (1996). II. The basal ganglia. In *Integrated Systems of the CNS: Cerebellum, Basal Ganglia, Olfactory System*, ed. Swanson LW, Bjorklund A & Hokfelt T. Elsevier, Amsterdam, pp. 371–457.

Im SH, Yu JH, Park ES, Lee JE, Kim HO, Park KI, Kim GW, Park CI & Cho SR (2010). Induction of striatal neurogenesis enhances functional recovery in an adult animal model of neonatal hypoxic-ischemic brain injury. *Neuroscience* **169**, 259–268.

Inta D, Alfonso J, von Engelhardt J, Kreuzberg MM, Meyer AH, van Hooft JA & Monyer H (2008). Neurogenesis and widespread forebrain migration of distinct GABAergic neurons from the postnatal subventricular zone. *Proc Natl Acad Sci U S A* **105**, 20994–20999.

Irvin DK, Kirik D, Bjorklund A & Thompson LH (2008). In vivo gene delivery to proliferating cells in the striatum generated in response to a 6-hydroxydopamine lesion of the nigro-striatal dopamine pathway. *Neurobiol Dis* **30**, 343–352.

Iwai M, Cao G, Yin W, Stetler RA, Liu J & Chen J (2007). Erythropoietin promotes neuronal replacement through revascularization and neurogenesis after neonatal hypoxia/ischemia in rats. *Stroke* **38**, 2795–2803.

Janavs JL & Aminoff MJ (1998). Dystonia and chorea in acquired systemic disorders. *J Neurol Neurosurg Psychiatry* **65**, 436–445.

Lange H, Thorner G, Hopf A & Schroder KF (1976). Morphometric studies of the neuropathological changes in choreatic diseases. *J Neurol Sci* **28**, 401–425.

Liu F, You Y, Li X, Ma T, Nie Y, Wei B, Li T, Lin H & Yang Z (2009). Brain injury does not alter the intrinsic differentiation potential of adult neuroblasts. *J Neurosci* **29**, 5075–5087.

Luskin MB (1993). Restricted proliferation and migration of postnatally generated neurons derived from the forebrain subventricular zone. *Neuron* **11**, 173–189.

Luzzati F, De Marchis S, Fasolo A & Peretto P (2006). Neurogenesis in the caudate nucleus of the adult rabbit. *J Neurosci* **26**, 609–621.

Maciejewska B, Lipowska M, Kowianski P, Domaradzka-Pytel B & Morys J (1998). Postnatal development of the rat striatum–a study using in situ DNA end labelling technique. *Acta Neurobiol Exp (Wars)* **58**, 23–28.

Mallard EC, Waldvogel HJ, Williams CE, Faull RL & Gluckman PD (1995). Repeated asphyxia causes loss of striatal projection neurons in the fetal sheep brain. *Neuroscience* **65**, 827–836.

Merkle FT, Mirzadeh Z & Alvarez-Buylla A (2007). Mosaic organization of neural stem cells in the adult brain. *Science* **317**, 381–384.

Olsson M, Campbell K, Wictorin K & Bjorklund A (1995). Projection neurons in fetal striatal transplants are predominantly derived from the lateral ganglionic eminence. *Neuroscience* **69**, 1169–1182.

Parent JM, Vexler ZS, Gong C, Derugin N & Ferriero DM (2002). Rat forebrain neurogenesis and striatal neuron replacement after focal stroke. *Ann Neurol* **52**, 802–813.

Plane JM, Liu R, Wang TW, Silverstein FS & Parent JM (2004). Neonatal hypoxic-ischemic injury increases forebrain subventricular zone neurogenesis in the mouse. *Neurobiol Dis* **16**, 585–595.

Reiner A, Albin RL, Anderson KD, D'Amato CJ, Penney JB & Young AB (1988). Differential loss of striatal projection neurons in Huntington disease. *Proc Natl Acad Sci U S A* **85**, 5733–5737.

Sanai N, Nguyen T, Ihrie RA, Mirzadeh Z, Tsai HH, Wong M, Gupta N, Berger MS, Huang E, Garcia-Verdugo JM, Rowitch DH & Alvarez-Buylla A (2011). Corridors of migrating neurons in the human brain and their decline during infancy. *Nature* **478**, 382–386.

Stenman J, Toresson H & Campbell K (2003). Identification of two distinct progenitor populations in the lateral ganglionic eminence: implications for striatal and olfactory bulb neurogenesis. *J Neurosci* **23**, 167–174.

Stopczynski RE, Poloskey SL & Haber SN (2008). Cell proliferation in the striatum during postnatal development: preferential distribution in subregions of the ventral striatum. *Brain Struct Funct* **213**, 119–127.

Sui Y, Horne MK & Stanic D (2012). Reduced proliferation in the adult mouse subventricular zone increases survival of olfactory bulb interneurons. *PLoS One* **7**, e31549.

Thompson L, Barraud P, Andersson E, Kirik D & Bjorklund A (2005). Identification of dopaminergic neurons of nigral and ventral tegmental area subtypes in grafts of fetal ventral mesencephalon based on cell morphology, protein expression, and efferent projections. *J Neurosci* **25**, 6467–6477.

Titomanlio L, Kavelaars A, Dalous J, Mani S, El Ghouzzi V, Heijnen C, Baud O & Gressens P (2011). Stem cell therapy for neonatal brain injury: perspectives and challenges. *Ann Neurol* **70**, 698–712.

van der Kooy D & Fishell G (1987). Neuronal birthdate underlies the development of striatal compartments. *Brain Res* **401**, 155–161.

Wichterle H, Turnbull DH, Nery S, Fishell G & Alvarez-Buylla A (2001). In utero fate mapping reveals distinct migratory pathways and fates of neurons born in the mammalian basal forebrain. *Development* **128**, 3759–3771.

Yang Z, You Y & Levison SW (2008). Neonatal hypoxic/ischemic brain injury induces production of calretinin-expressing interneurons in the striatum. *J Comp Neurol* **511**, 19–33.

Author contributions

Acknowledgements